Supplementary Table 1. Input features for GFP 'on-target' model selection.

	Feature Name	Description
1	crRNA MFE	Minimum free energy value of DR-sequence plus guide sequence using `RNAfold`
2	direct repeat	Binary - based on the presence of the predicted DR fold "((((((.(((....))).))))))" at the crRNA start
3	G-quadruplex	Binary - based on the presence of the predicted G-quadruplex indicated by "+" within the folding sequence
4	hybMFE 1:26	Minimum free energy value between guide RNA nucleotides 1-26 and its corresponding target site (=overall hybridization)
5	hybMFE 1:10	Minimum free energy value between guide RNA nucleotides 1-10 and its corresponding target site (=5' hybridization)
6	hybMFE 19:8	Minimum free energy value between guide RNA nucleotides 19-27 and its corresponding target site (=3' hybridization)
7	$\log_{10}$(Unpaired prob1)	$\log_{10}$(probability) of a target RNA nucleotide being unpaired in a window centered at nt -23 relative to the guide match start summarizing 21 nts (nt -13:-33)
8	$\log_{10}$(Unpaired prob2)	$\log_{10}$(probability) of a target RNA nucleotide being unpaired in a window centered at nt -23 relative to the guide match start summarizing 10 nts (nt -27:-18)
9	A1 context	Probability of target RNA A-bases at position -22 relative to the guide match start summarizing 7 nts (nt -19:-25)
10	A2 context	Probability of target RNA A-bases at position -22 relative to the guide match start summarizing 33 nts (nt -6:-48)
11	A3 context	Probability of target RNA A-bases at position -16 relative to the guide match start summarizing 20 nts (nt -25:-6)
12	C context	Probability of target RNA C-bases at position -11 relative to the guide match start summarizing 22 nts (nt -21:0)
13	G context	Probability of target RNA G-bases at position -10 relative to the guide match start summarizing 21 nts (nt 20:0)
14	U context	Probability of target RNA U-bases at position -3 relative to the guide match start summarizing 18 nts (nt -12:+5)
15	upstream U context	Probability of target RNA U-bases at position -78 relative to the guide match start summarizing 30 nts (nt -93:-64)

For the RF_{GFP} model we define features as follows: For guide RNA features (features **4**, **5**, **6**), nucleotide 1 defines the guide match start site (GSS) being the most 5' guide RNA base matching the target RNA. Nucleotide 2 relative to GSS is the subsequent base (moving in the 5' to 3' direction) in the guide RNA and so on. For target RNA features (features **7** – **15**), we denote the target nucleotide opposite to the GSS as nucleotide 0. Moving in 5' to 3' direction target RNA nucleotide -1 is upstream (5') to target RNA nucleotide 0 and base-paired to guide nucleotide 2, while target RNA nucleotide +1 is downstream of the target site and so on. A complete illustration for features **4** – **15** with a schematic of the guide RNA and target RNA can be found in Supplementary Note 1, Figure 6.

Supplementary Table 2. Selected Input features for $RF_{combined}$ 'on-target' model.

	Feature Name	Description
1	crRNA MFE	Minimum free energy value of DR-sequence plus guide sequence using `RNAfold`
2	Direct repeat	Binary - based on the presence of the predicted DR fold "((((((.(((....))).))))))" at the crRNA start
3	G-quadruplex	Binary - based on the presence of the predicted G-quadruplex indicated by "+" within the folding sequence
4	HybMFE 3:15	Minimum free energy value between guide RNA nucleotides 3-15 and its corresponding target site (=5' hybridization)
5	HybMFE 15:23	Minimum free energy value between guide RNA nucleotides 15-23 and its corresponding target site (=3' hybridization)
6	Log_{10}(Unpaired prob)	log_{10}(probability) of a target RNA nucleotide being unpaired in a window centered at nt -11 relative to the guide match start summarizing 23 nts (nt 0:-22)
7	Local A_{max} probability	Probability of target RNA A-bases at position -10 relative to the guide match start summarizing 8 nts (nt -14:-7)
8	Local C_{max} probability	Probability of target RNA C-bases at position -16 relative to the guide match start summarizing 4 nts (nt -18:-15)
9	Local G_{max} probability	Probability of target RNA G-bases at position -19 relative to the guide match start summarizing 3 nts (nt -20:-18)
10	Local U_{max} probability	Probability of target RNA U-bases at position -6 relative to the guide match start summarizing 12 nts (nt -12:-1)
11	Local AU_{max} probability	Probability of target RNA A or U-bases at position -7 relative to the guide match start summarizing 11 nts (nt -12:-2)
12	Local GC_{max} probability	Probability of target RNA G or C-bases at position -18 relative to the guide match start summarizing 9 nts (nt -22:14)
13	Local A_{min} probability	Probability of target RNA A-bases at position -17 relative to the guide match start summarizing 7 nts (nt -20:-14)
14	Local C_{min} probability	Probability of target RNA C-bases at position -3 relative to the guide match start summarizing 9 nts (nt -7:+1)
15	Local G_{min} probability	Probability of target RNA G-bases at position -9 relative to the guide match start summarizing 9 nts (nt -13:-5)
16	Local U_{min} probability	Probability of target RNA U-bases at position -17 relative to the guide match start summarizing 10 nts (nt -22:-13)
17	Local AU_{min} probability	Probability of target RNA A or U-bases at position -17 relative to the guide match start summarizing 9 nts (nt -21:-13)
18	Local GC_{min} probability	Probability of target RNA G or C-bases at position -18 relative to the guide match start summarizing 11 nts (nt -11:-1) (GC_{min} - *not used in* $RF_{combined}$)
19-22	Nucleotide probability	Probability of guide RNA A,C, G or U bases (U - *not used in* $RF_{combined}$)
23-38	Di-nucleotide probability	Probability of 16 possible guide RNA di-nucleotides (UU - *not used in* $RF_{combined}$)

For the $RF_{combined}$ model we define features as follows: For guide RNA features (features **4** and **5**), nucleotide 1 defines the guide match start site (GSS) being the most 5' guide RNA base matching the target RNA. Nucleotide 2 relative to GSS is the subsequent base (moving in the 5' to 3' direction) in the guide RNA and so on. For target RNA features (features **6** – **18**), we denote the target nucleotide opposite to the GSS as nucleotide 0. Moving in 5' to 3' direction target RNA nucleotide -1 is upstream (5') to target RNA nucleotide 0 and base-paired to guide nucleotide 2, while target RNA nucleotide +1 is downstream of the target site and so on. A complete illustration for features **4** – **18** with a schematic of the guide RNA and target RNA can be found in Supplementary Note 2, Figure 6.

Supplementary Note 1

Features of Cas13d targeting from the GFP tiling screen

Anti-Tag

Recently, others have found that Cas13a is inhibited by a 4 nt "anti-tag" sequence — homology between the end of the DR and the corresponding flanking sequence of the target — and have speculated that Cas13d, which has a similarly positioned 5' DR, might also use an anti-tag for host versus pathogen discrimination [1]. Using all perfect match guide RNAs, we did not find evidence for the presence of a similar anti-tag sequence for *Rfx*Cas13d suggesting that anti-tags may not be found in all Type VI CRISPRs or contribute only marginally compared to other features (**Note 1 Fig. 1**).

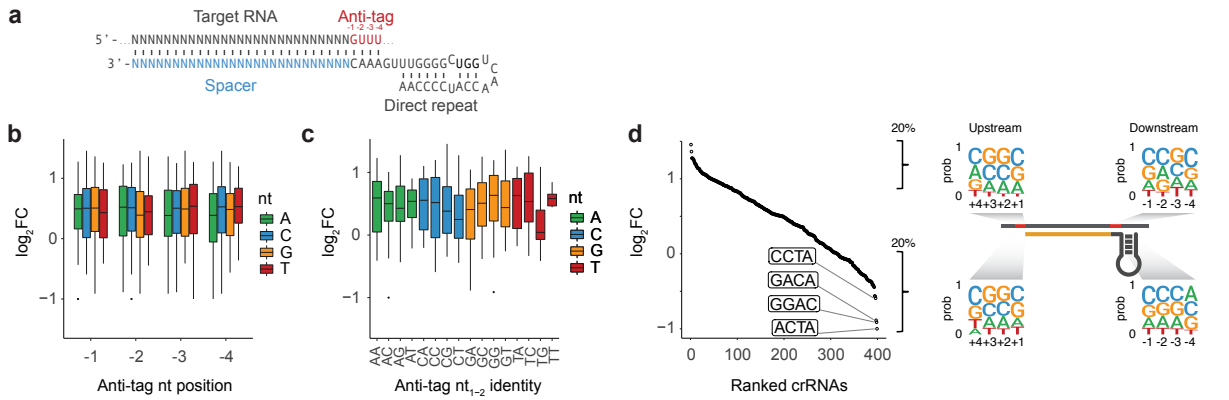

Note 1 Figure 1. No evidence for the presence of an *Rfx*Cas13d anti-tag in GFP tiling screen. (**a**) Anti-tag position in target RNA. (**b**) Log_2FC of all perfect match guides (n = 399) segregated by anti-tag nucleotide identity at anti-tag positions 1 through 4. (**c**) Same as in *b*, but segregated by anti-tag di-nucleotide identity at anti-tag positions 1 and 2 (**d**) (*left*) log_2FC-ranked guide RNAs (n = 399) highlighting the anti-tag sequence for the 4 least efficient guides. (*right*) Position Weight Matrices (PWMs) depicting the positional nucleotide probabilities of either the top 20% or bottom 20% log_2FC-ranked guides 5' and 3' (i.e. putative anti-tag) relative to the guide RNA match position. Boxes in *b* and *c* indicate the median and interquartile ranges, with whiskers indicating 1.5 times the interquartile range, or the most extreme data point outside the 1.5-fold interquartile.

Nucleotide preferences

Next, we tested whether position-based nucleotide preferences exist within the guide RNA target sequence or nearby nucleotides by comparing the nucleotide composition of the top 20% to all perfectly matching guides in the GFP screen, similar to previous approaches assessing Cas9 guide preferences [2]. Although the top enriched guides showed slight nucleotide preferences compared to all guides, most preferences became insignificant after correction for multiple hypothesis testing (**Note 1 Fig. 2a**). However, when we correlated guide RNA nucleotide probabilities with the observed guide enrichment, we saw that high 'G'-content in the guide RNA had a strong negative impact (**Note 1 Fig. 2b-c**). Other measures, like guide RNA GC-content indicated a local optimum around 50% with lower guide efficiency when the guide adopts lower or higher GC proportions.

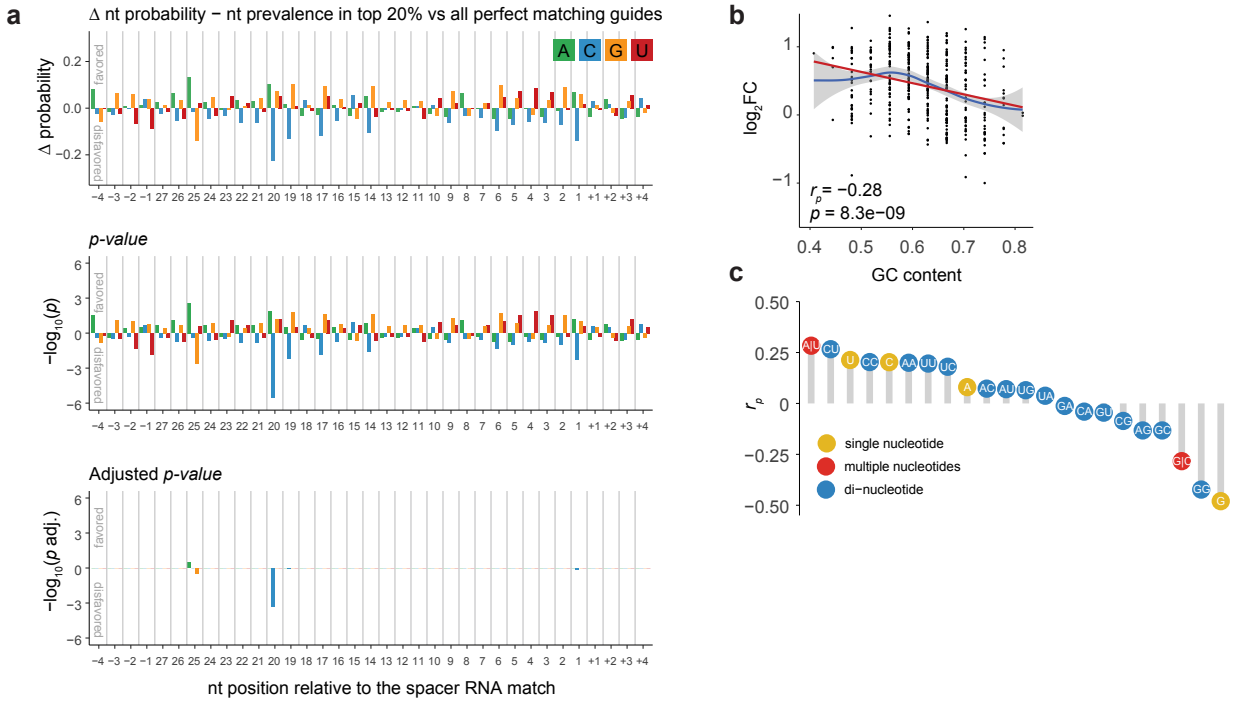

Note 1 Figure 2. Cas13d guide RNA nucleotide preferences influence guide RNA efficacies in GFP screen. (**a**) (*top*) Effect-size (delta nucleotide probabilities), (*middle*) *p*-values and (*bottom*) Bonferroni-corrected *p*-values of observing the conditional probability of a guide in the top 20% under the null distribution examined at every position including the 4 nucleotides 5' and 3' of the guide RNA target site. The *p*-values were calculated from the binomial distribution with a baseline probability estimated from the full-length mRNA target sequence with all perfect match guide RNAs (n = 399) (**b**) Scatterplot depicting the guide RNA $\log_2$FC and guide RNA GC-content as a fraction (n = 399). The red line indicates the linear relationship between both values (Pearson correlation coefficient r_p, p = 8.3e-09). The blue line indicates a LOESS fit and has a local optimum around a GC-content of 0.5-0.6. (Grey shading denotes LOESS fit confidence interval) (**c**) As in *b*, but showing the Pearson correlation coefficient (r_p) between guide RNA $\log_2$FC and all guide single nucleotides, di-nucleotides, and G|C and A|U-content.

crRNA folding

The negative correlation to the observed guide RNA enrichments ($\log_2$FC) was restricted to high 'G'-content in the guide RNA, while guide RNA 'C'-content did not affect targeting in the same way (**Note 1 Fig. 2c**). This suggests that the effect may not be caused by specific guide-target interaction, which should weight 'C' and 'G' bases interchangeably, but instead may be driven by 'G'-dependent stable structures within the crRNA that may render the crRNA inaccessible for Cas13d. Indeed, predicting the secondary structure and corresponding minimum free energy (MFE) of perfect match guides showed a positive correlation between the MFE and guide efficacy (**Supplementary Fig. 6a**). In particular, 'G'-dependent structures, such as predicted G-quadruplexes, showed diminished target knock-down.

Guide RNA – target RNA hybridization

We next tested whether guide-target hybridization can contribute to guide RNA efficacy by computing the correlation between hybridization energy and guide RNA efficacy (**Note 1 Fig. 3a**). For the GFP screen we found that more stable hybridization between guide RNAs and their target

sequences (lower MFE) was correlated with lower guide RNA efficacy (r = 0.31) (**Note 1 Fig. 3b**). This suggests that the most stable guide-target interactions may render the ribonucleoprotein complex less active. Interestingly, calculating MFEs between smaller regions within the guide RNA indicated multiple sub-structures that contribute to the overall correlation, suggesting that individual parts of the guide-target interaction may serve specific roles during ternary complex formation or nuclease activation (**Note 1 Fig. 3a**). However, these correlative structures were nearly gone when using partial correlation to control for the effect of crRNA folding (**Note 1 Fig. 3c**).

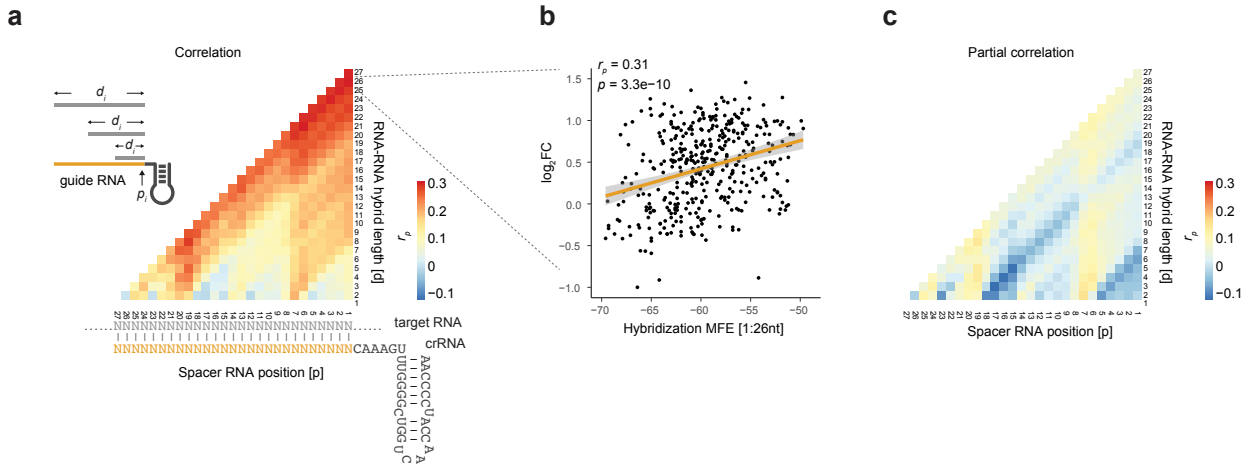

Note 1 Figure 3. Hybridization energy between guide RNA and target site sequence. (**a**) Pearson correlation coefficient (r_p) of the observed log$_2$FC and the hybridization minimum free energy (MFE) of guide RNA nucleotide position p over the distance d to the position p+d with its cognate target sequence for all perfectly matching guide RNAs (n = 399 for each cell) (**b**) Example scatterplot of a showing the linear relationship (*line* = Pearson correlation coefficient r_p, p = 3.3e-10, n = 399) between the observed log$_2$FC and the hybridization MFE of guide RNA nucleotides 1-26 and its cognate target sites for all perfectly matching guide RNAs. (Grey shading denotes the linear fit confidence interval) (**c**) As in a, but using partial Pearson correlations controlling for the crRNA MFE as shown in **Supplementary Fig. 6a**. The same r_p scale is used for panels a and c.

Target site nucleotide context

Beyond guide RNA nucleotide composition, we wondered if the context features of the guide RNA target site affected target knock-down. By correlating the observed guide RNA log$_2$FC with the nucleotide probabilities across windows around target sites, we detected a strong negative impact of high 'C'-context directly at the target site (**Note 1 Fig. 4** *left*). However, this may be confounded by the high guide RNA 'G'-content and its role in crRNA folding (**Supplementary Fig. 6**). Indeed, using partial correlation to account for the crRNA MFE diminished the negative correlation strength (**Note 1 Fig. 4** *right*). Outside the direct target site, we noticed that high 'U'-content upstream (5') to the target site positively correlated with target knock-down, which is consistent with previous reports of higher nuclease activity in 'U'-rich contexts [3,4] (**Note 1 Fig. 4**). In order to understand if the observed upstream U-context is generalizable or targeting position specific, we generated a GFP reporter plasmid that allowed for changing the nucleotide context upstream of a perfect match target site. We designed a 52mer oligonucleotide lacking uridines and optimized to minimize predicted RNA secondary structures. We cloned this and 52mer oligonucleotides with 3 or 6 uridines at various positions into the GFP-reporter plasmid and tested the upstream uridine

context effect on target knock-down. Each reporter was targeted directly downstream of the introduced oligo, or with a non-targeting guide. This was done, because the introduced uridines could potentially act as cis-regulatory elements and recruit RNA binding proteins and thus influence target RNA stability independent of the Cas13 protein [5]. We did not observe a significant position dependent effect of the upstream (5') uridines (**Note 1 Fig 4b-c**), suggesting that the effect may be target site specific, driven by additional downstream U content or too weak to be assessed in this experiment.

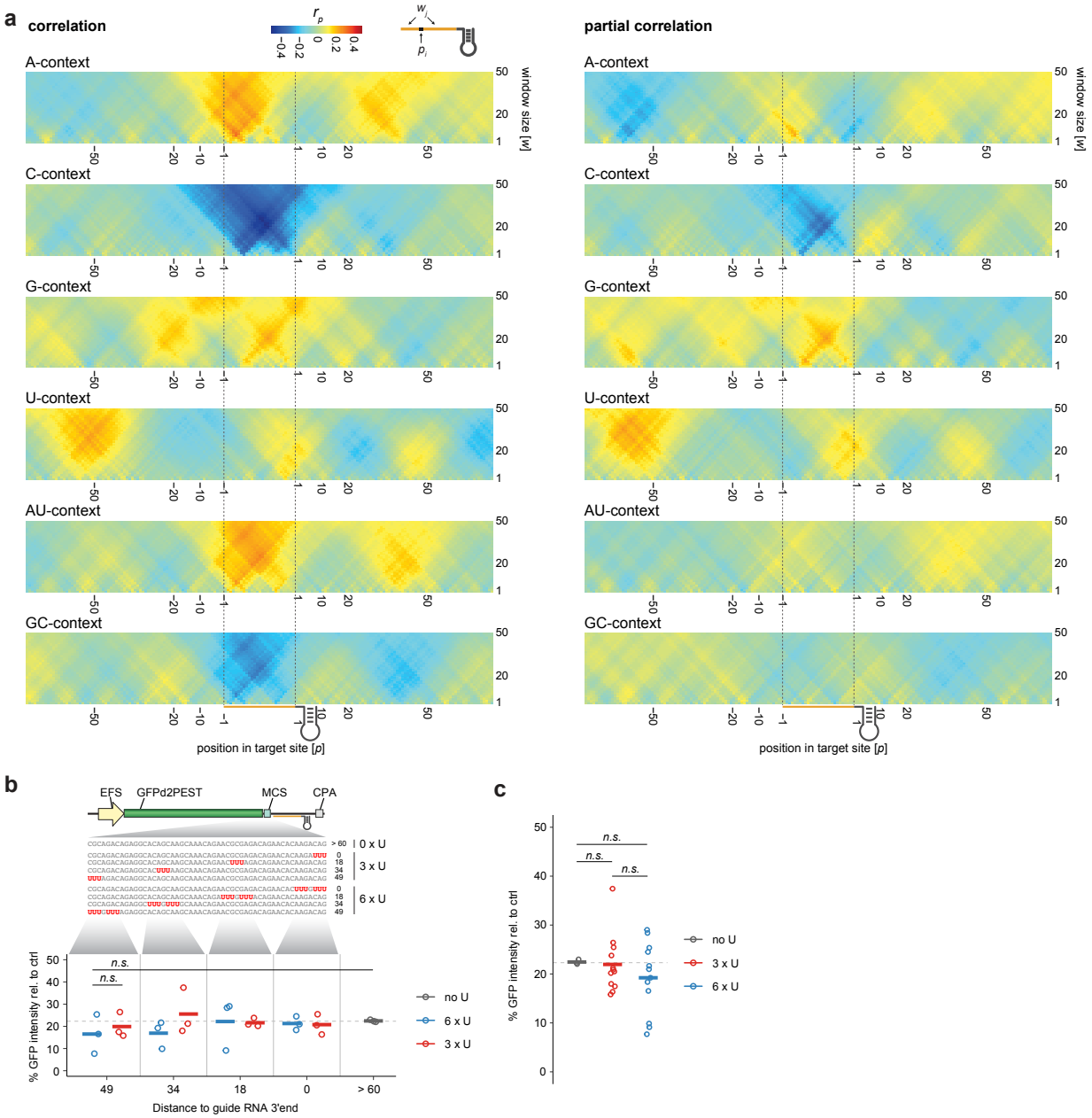

Note 1 Figure 4. Local target sequence context of GFP transcript targeting guides. (**a**) Heatmaps depicting the Pearson correlation coefficient (r_p) between the local target nucleotide-contexts (A, C, G, U, A|U and G|C) and observed log_2FC relative to guide RNA match positions. We performed a grid-search correlating the observed crRNA efficacies with the summarized target nucleotide density across a window of 1 nt up to 50 nt at every point 75 nt 5' of the target site to 75 nt 3' of the target site (n = 399 for each cell). (*left*) Pearson correlation coefficient, (*right*) partial

Pearson correlation controlling for the crRNA MFE as shown in **Supplementary Fig. 6**. (**b**) Target knock-down comparison varying the upstream uridine context (position and number of uridine residues) relative to the guide RNA target site. The 60 nucleotides upstream sequence contained either 0, 3 or 6 uridines at positions 49, 34, 18 or 0 nucleotides upstream of a 26mer guide RNA. *Rfx*Cas13d-NLS expressing cells were co-transfected with plasmids delivering the crRNA and with a GFP-encoding reporter plasmid. Shown is the percentage of mean fluorescence intensity reduction of cells transfected with a GFP-targeting guide relative to a non-targeting guide. The bar represents the mean of three biological replicate experiments. (**c**) As in *b* but split by number of uridines within the upstream 60 nucleotides. Differences between 0, 3 and 6 Us at each individual position, as well as summarized across all positions were not significant using one-tailed *t*-test.

Target site accessibility

We also assessed whether the target site accessibility influences knock-down by correlating the observed guide RNA efficacies with the target site accessibility. Here, we define target site accessibility as the probability that the target RNA (in this case, GFP mRNA) is unpaired. We found a weak positive correlation with increased target site accessibility centered on the 3'-end of the spacer RNA (**Note 1 Fig. 5**) reminiscent of target-RNA accessibility preferences shown for Cas13b [6].

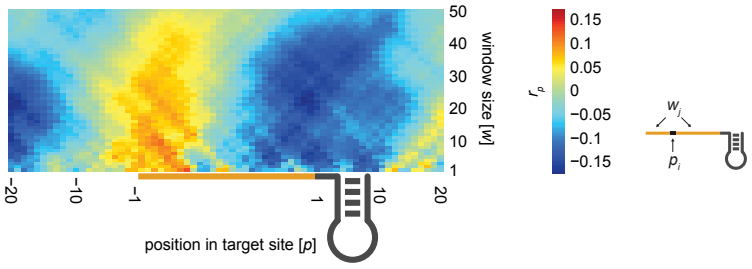

Note 1 Figure 5. Target site accessibility. Heatmap depicting the Pearson correlation coefficient (r_p) between the local target site accessibility (= $\log_{10}$(unpaired probability)) and the observed $\log_2$FC relative to guide RNA match positions. We performed a grid-search correlating the observed guide RNA efficacies with the unpaired probability in a window (w) of 1 nt up to 50 nt at every point 20 nt 5' of the target site to 20 nt 3' of the target site (n = 399 for each cell).

On-target model feature collection

Based on our analyses above, we determined the position and window-size with the best correlation to the observed guide RNA enrichments for each feature (**Note 1 Fig. 6**). A full list of all features evaluated in the on-target model based in the GFP-tilling screen data can be found in **Supplementary Table 1**.

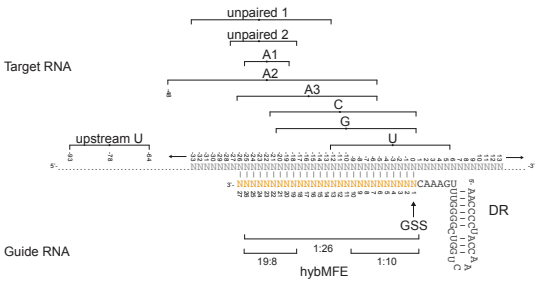

Note 1 Figure 6. Overview of guide RNA and target RNA feature windows. For guide RNA features nucleotide 1 defines the guide match start site (GSS) being the most 5' guide RNA base matching the target RNA. Nucleotide 2 relative to GSS is the subsequent base (moving in the 5' to 3' direction) in the guide RNA and so on. For target RNA features, we denote the target nucleotide opposite to the GSS as nucleotide 0. Moving in 5' to 3' direction target RNA nucleotide -1 is upstream to the GSS and pairs with guide nucleotide 2, while target RNA nucleotide +1 is downstream of the target site and so on.

Supplementary Note 2

Features of Cas13d targeting from combined tiling screens

For the assessment of crRNA and target RNA features, we considered 2,918 perfect match guides that target coding regions across four genes: GFP, CD46, CD55, CD71 (see **Fig. 1d** and **Fig. 3a-c**). Compared to the 399 perfect-match guide RNAs from the GFP screen alone, this represents a 7.3-fold increase in data points. To make the screens more comparable, we scaled the log_2FC of each screen independently. We preferred scaling each dataset over assigning ranks between 1 and 0 in order to maintain relative guide strength differences between screens, under the assumption that the strongest guide in screen *A* may not be as strong as the strongest guide in screen *B*. Here, each feature is represented across all 4 screens. In addition to this combined analysis, analyses for each independent screen can be found on our *gitlab* repository (https://gitlab.com/sanjanalab/cas13).

Anti-Tag

Using all perfect match guide RNAs, we did not find evidence for the presence of an anti-tag sequence[1] for *Rfx*Cas13d suggesting that anti-tags may not be found in all Type VI CRISPRs or contribute only marginally compared to other features (**Note 2 Fig. 1**).

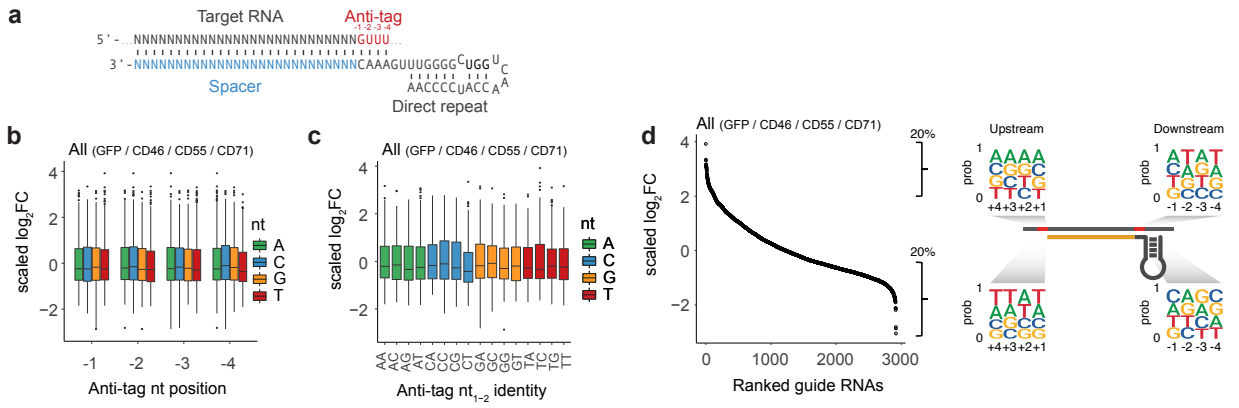

Note 2 Figure 7. Combined screen shows no evidence for the presence of an *Rfx*Cas13d anti-tag. (**a**) Anti-tag position in target RNA. (**b**) Log_2FC of all perfect match guide RNAs (n = 2,918) segregated by anti-tag nucleotide identity at anti-tag positions 1 through 4. (**c**) Same as in *b*, but segregated by anti-tag di-nucleotide identity at anti-tag positions 1 and 2 (**d**) (*left*) log_2FC-ranked guide RNAs highlighting the anti-tag sequence for the 4 least efficient guides (n = 2,918). (*right*) Position Weight Matrices (PWMs) depicting the positional nucleotide probabilities of either the top 20% or bottom 20% log_2FC-ranked guides upstream and downstream (i.e. anti-tag) relative to the guide RNA match position. (The 20% selection was applied to each screen separately to ensure equal contribution). Boxes in *b* and *c* indicate the median and interquartile ranges, with whiskers indicating 1.5 times the interquartile range, or the most extreme data point outside the 1.5-fold interquartile.

Nucleotide preferences

Next, we tested whether position-based nucleotide preferences exist within the guide RNA target sequence or nearby nucleotides by comparing the nucleotide composition of the top 20% to all perfectly matching guides across all four screens, similar to previous approaches assessing Cas9

guide preferences [2]. The increased number of data points uncovered clear nucleotide preferences (**Note 2 Fig. 2a**). The top enriched guides showed preferences for G-bases at guide nucleotides 19 – 21 (with position 1 defined as the most 5' nucleotide in the guide RNA that matches the target RNA). C-bases were favored at positions 15 – 16. Interestingly, the enrichment of G and C bases surround the center of the critical seed region at position 18 (see **Fig. 1f**). Moreover, we observed before that increased GC-content surrounding mismatches at position 18 correlated with the relative decrease in guide efficiency (delta $\log_2$FC). This suggested that increased high GC-content may ameliorate the effect size of mismatches in the seed region (compare **Supplementary Fig. 5**). There was also a mild enrichment for A- and U-bases in the first half of the guide RNA.

We correlated guide RNA nucleotide probabilities with the observed guide enrichment. In the GFP screen data alone we found that high 'G'-content in the guide RNA had a strong negative impact. This impact was reduced when taking all four screens into account (**Note 2 Fig. 2b-c**). The guide RNA GC-content indicated a local optimum around 50% with lower guide efficiency when the guide adopts lower or higher GC proportions.

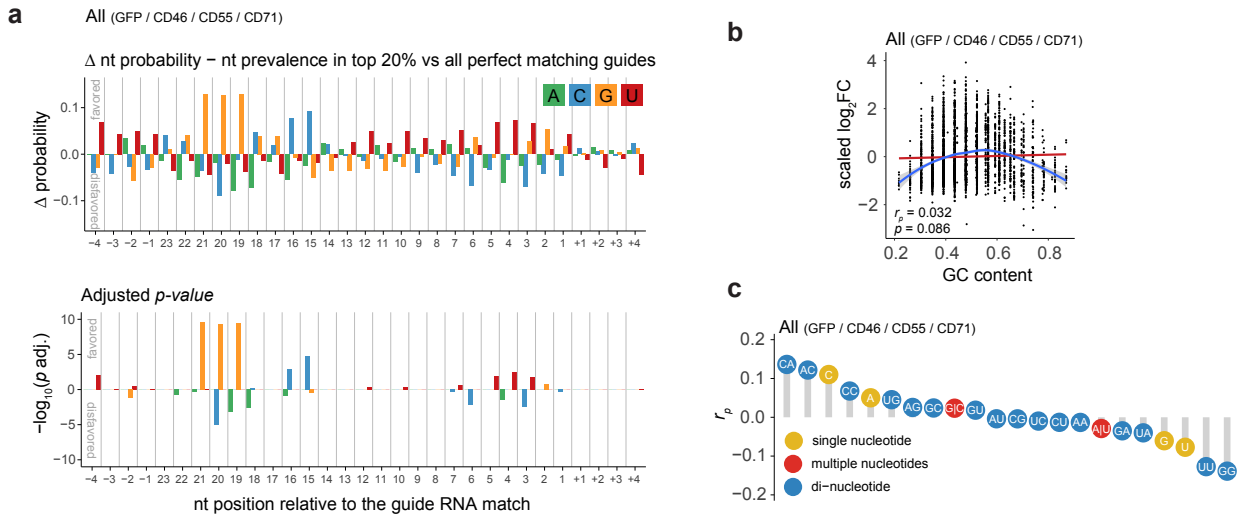

Note 2 Figure 8. Cas13d guide RNA nucleotide preferences influence guide RNA efficacies across all screens. (**a**) (*top*) Effect-size (delta nucleotide probabilities) and (*bottom*) Bonferroni-corrected *p*-values of observing the conditional probability of a guide in the top 20% under the null distribution examined at every position including the 4 nucleotides upstream and downstream of the guide RNA target site. The *p*-values were calculated from the binomial distribution with a baseline probability estimated from the full-length mRNA target sequence all perfect match guide RNAs (tow-sided). The top 20% were selected for each screen separately to ensure equal contribution ($n = 2{,}918$). (**b**) Scatterplot depicting the guide RNA $\log_2$FC (*y*-axis) and guide RNA GC-content as a fraction of guide length ($n = 2{,}918$). The red line indicates the linear relationship between both values (Pearson correlation coefficient r_p,$p = 0.086$). The blue line indicates a LOESS fit and has a local optimum around a GC-content of 0.5 (Grey shading denotes LOESS fit confidence interval). (**c**) As in *b*, but showing the Pearson correlation coefficient (r_p) between guide RNA $\log_2$FC and all guide single nucleotides, di-nucleotides, and G|C and A|U-content.

crRNA folding

Analyzing the GFP screen alone, we found previously that the predicted crRNA folding minimum free energy (MFE) of perfect match guides correlated positively with guide RNA efficacy (see **Supplementary Fig. 6a**). Low MFE values were associated with low guide RNA efficiencies suggesting that stable crRNA folds may hinder crRNA utilization by Cas13d. Extending this analysis to perfect match guide RNAs of all screen, we observed an overall decrease in the correlation between crRNA MFE and guide efficiency (**Note 2 Fig. 3**). However, low MFEs still associated with low guide RNA efficiencies. Additional predicted G-quadruplex structures were not observed in the CD46, CD55 and CD71 screens.

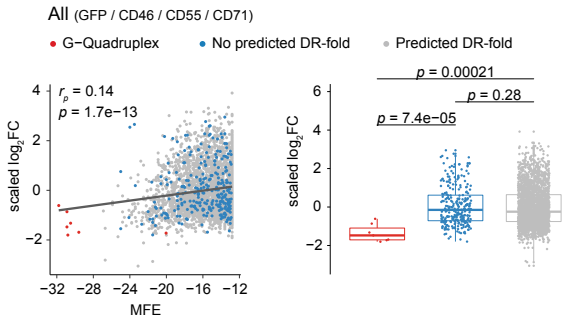

Note 2 Figure 9. Proper folding of the direct repeat affects crRNA targeting efficacy. (a) Scatterplot showing the scaled guide RNA log_2FC versus the predicted crRNA secondary structure minimum free energy (MFE). The Pearson correlation coefficient (r_p) is nearly unchanged (r_p = 0.12) when MFEs of G-quadruplex-forming crRNAs are ignored. (All *n* = 2,918, Predicted DR-fold *n* = 2,634, No predicted DR-fold *n* = 278, predicted G-quadruplex *n* = 7; two-sided *t*-test). Boxes indicate the median and interquartile ranges, with whiskers indicating 1.5 times the interquartile range.

Guide RNA – target RNA hybridization

We next tested whether guide-target hybridization can contribute to guide RNA efficacy when integrating data from all four screens. Unlike for the GFP screen alone, we found that the overall hybridization energy between the full-length guide RNA and target sequence correlated less (**Note 2 Fig. 4a**). Instead, the hybridization energies of sub-fragments contributed differentially to the overall guide-target interaction. The hybridization energy between the 12 nucleotides from guide position 3 to 15 and the cognate target site showed a slight positive correlation (**Note 2 Fig. 4a-b**). Hybridization energies covering the 9 nucleotides from guide position 15 to 23 correlated negatively with the knock-down efficiencies (**Note 2 Fig. 4a-b**). Unlike for the GFP screen analysis before, these sub-structures were still present when controlled for the crRNA folding energies using partial correlations (**Note 2 Fig. 4c**).

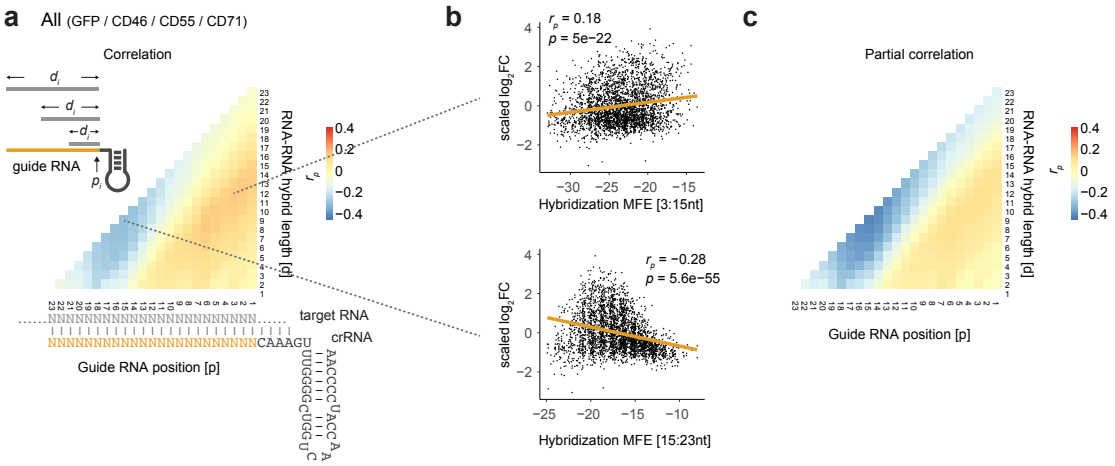

Note 2 Figure 10. Hybridization energy between guide RNA and target site sequence. (**a**) Pearson correlation coefficient (r_p) of the observed scaled $\log_2$FC and the hybridization minimum free energy (MFE) of guide RNA nucleotide position *p* over the distance *d* to the position *p*+*d* with its cognate target sequence for all perfectly matching guide RNAs (n = 2,918 for each cell). (**b**) Example scatterplot of *a* showing the linear relationship between the observed scaled $\log_2$FC and the hybridization MFE of guide RNA nucleotides 3-15 (*top*) and 15-23 (*bottom*) and their cognate target sites for all perfectly matching guide RNAs (*line* = Pearson correlation coefficient r_p, n = 2,918) (**c**) As in *a*, but using partial Pearson correlations controlling for the crRNA MFE as shown in **Note 2 Fig. 3** (n = 2,918 for each cell). The same r_p scale is used for panels *a* and *c*.

Target site accessibility

We also assessed the target site accessibility for all screens and correlated observed guide RNA efficacies with the target site accessibility. Here, we define target site accessibility as the probability that the target RNA is unpaired. We did not find a strong relationship between the probability of the target sequence being unpaired and the observed knock-down strengths (**Note 2 Fig. 5**). Similar to the GFP screen alone, we find a weak positive correlation with increased target site accessibility centered on the 3'-end of the spacer RNA. We also recapitulate the observed nucleotide preferences with higher GC-content centered around seed nucleotide 18, which is surrounded by higher AU-content (compare **Supplementary Figure 10a-b**). Higher AU-content translates to increased accessibility, while higher GC content suggest local secondary structures.

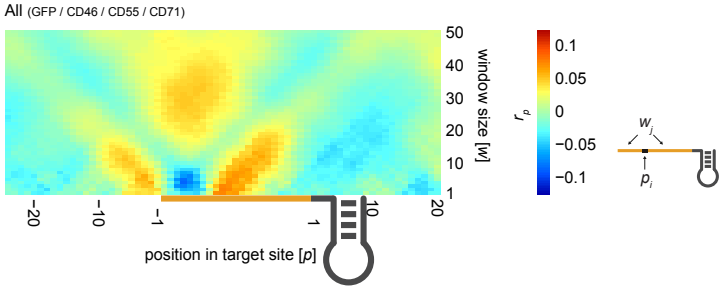

Note 2 Figure 11. Target site accessibility. Heatmap depicting the Pearson correlation coefficient (r_p) between the local target site accessibility (= $\log_{10}$(unpaired probability)) and the observed $\log_2$FC relative to guide RNA match positions. We performed a grid-search correlating the observed guide efficacies with the $\log_{10}$-transformed unpaired

probability in a window (*w*) of 1 nt up to 50 nt at every point 20 nt 5' of the target site to 20 nt 3' of the target site. (*n* = 2,918 for each cell).

On-target model feature collection

Based on our analyses across all four tiling screens, we determined the position and window-size with the best correlation to the observed guide RNA enrichments for each feature (**Note 2 Fig. 6**). For the RNA target site accessibility we chose the entire target site as a window instead of the weak positive correlation that correlated with the U-context in in that region (from nucleotide 1 – 23 with position 1 defined as the most 5' nucleotide in the guide RNA that matches the target RNA). A full list of all features evaluated in the on-target model based in the GFP-tilling screen data can be found in **Supplementary Table 2**.

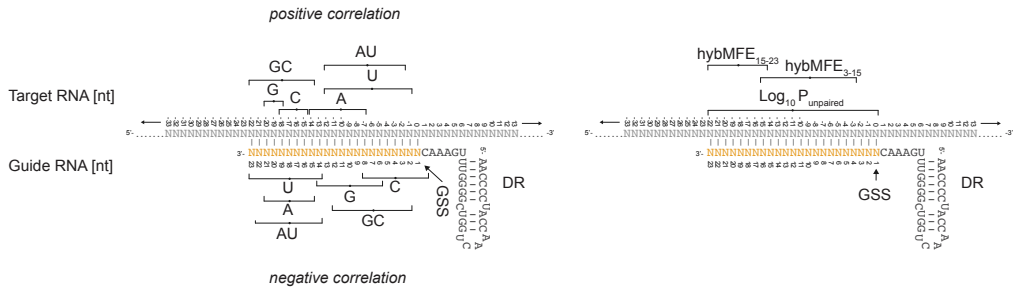

Note 2 Figure 12. Overview of guide RNA and target RNA feature windows. For guide RNA features nucleotide 1 defines the guide match start site (GSS) being the most 5' guide RNA base matching the target RNA. Nucleotide 2 relative to GSS is the subsequent base (moving in the 5' to 3' direction) in the guide RNA and so on. For target RNA features, we denote the target nucleotide opposite to the GSS as nucleotide 0. Moving in 5' to 3' direction target RNA nucleotide -1 is upstream to the GSS and pairs with guide nucleotide 2, while target RNA nucleotide +1 is downstream of the target site and so on. Selected features with either positive or negative correlation are denoted with the subscript 'max' or 'min', respectively, in **Supplementary Table 2**.

References

1. Meeske, A. J. & Marraffini, L. A. RNA Guide Complementarity Prevents Self-Targeting in Type VI CRISPR Systems. *Mol. Cell* **71**, 791–801 (2018).
2. Doench, J. G. *et al.* Rational design of highly active sgRNAs for CRISPR-Cas9-mediated gene inactivation. *Nat. Biotechnol.* **32**, 1262–1267 (2014).
3. Konermann, S. *et al.* Transcriptome Engineering with RNA-Targeting Article Transcriptome Engineering with RNA-Targeting. *Cell* **173**, 1–12 (2018).
4. Freije, C. A. *et al.* Programmable Inhibition and Detection of RNA Viruses Using Cas13. *Mol. Cell* **76**, 1–12 (2019).
5. Mukherjee, N. *et al.* Integrative regulatory mapping indicates that the RNA-binding protein HuR couples pre-mRNA processing and mRNA stability. *Mol. Cell* **43**, 327–39 (2011).
6. Smargon, A. A. *et al.* Cas13b Is a Type VI-B CRISPR-Associated RNA-Guided RNase Differentially Regulated by Accessory Proteins Csx27 and Csx28. *Mol. Cell* **65**, 618–630 (2017).